AD _____

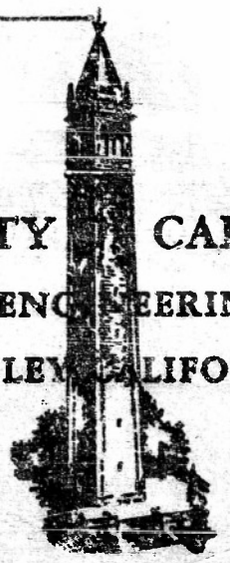

UNIVERSITY OF CALIFORNIA
INSTITUTE OF ENGINEERING RESEARCH
BERKELEY, CALIFORNIA

The Mechanics of Deep Water, Shallow Water, and Breaking Waves

By

Jack R. Morison and R. C. Crooke

SERIES NO. 3

ISSUE NO. 344

DATE February 1953

University of California
Department of Engineering
Submitted under contract N7onr 295(26)
with the Office of Naval Research (NR 083-088)

Institute of Engineering Research
Waves Research Laboratory
Technical Report
Series 3, Issue 344

The Mechanics of Deep Water, Shallow Water, and Breaking Waves

by

Jack R. Morison and R. C. Crooke

Berkeley, California
February 1953

Acknowledgement

This report was sponsored by the Office of Naval Research. The authors greatly appreciate the assistance of H. E. Chamberlain, W. L. Erdmann, R. D. Costello, E. K. Rice, D. M. Nelson, M. J. Larrocco, F. E. Mead, M. M. Lincoln, C. M. Lamont, and M. E. Conklin in the preparation of this report.

The Mechanics of Deep Water, Shallow Water, and Breaking Waves

Abstract - Experimental data are presented for deep water, shallow water, and breaking waves with respect to the wave surface time history, the horizontal and vertical particle velocities and the particle orbits. The measurements are compared where applicable to Stokes wave theory. The results are that the Stokes wave theory[1,2,3,4]*, and other wave theories[2,3,4], show good agreement with the measurements for deep water conditions and even to d/L values of approximately 0.2. The theories do not apply for shallow water conditions where d/L values are appreciably less than 0.2 and the waves have an appreciable steepness.

Introduction - The purpose of this report is to present experimental data on the mechanics of waves and to compare these data with the Stokes wave theory[1,2,3,4]. The wave surface time history, horizontal and vertical particle velocities and the particle orbit were measured in deep water, shallow water, and for breaking waves. The Stokes theory showed good agreement with the measurements for conditions where d/L was greater than about 0.2. For shallow water waves (d/L appreciably less than 0.2) of appreciable steepness and for breaking waves on sloping beaches, the Stokes theory to the second approximation shows poor agreement. It was found that steep waves near the breaking point on a steep beach will show closer agreement with the Stokes theory than low waves on a flat beach. The surface time history at the point of breaking shows close agreement with the space profile at a distance of 20% of the wave length on either side of the breaking point. The greatest horizontal particle velocity occurs when a wave breaks, but there is no evidence that any particles approach the wave velocity except the particles at the crest of the breaking wave. The greatest vertical velocity occurs in an upward direction, just as the wave breaks. For unbroken waves that are asymmetrical about the crest, the greatest vertical velocity occurs in an upward direction, just as the wave crest approaches the particle. Extremely shallow water waves in a channel form a second wave that travels at a slower velocity than the original wave, thus forming waves that do not have a permanent form. The particle orbit of this wave train consists of an ellipse within an ellipse if the second wave is in the trough of the original wave. No mass transport studies were attempted because of unknown tank effects.

Experiments - The experiments were conducted in the 1 ft. by 3 ft. by 60 ft. wave channel in the Fluid Mechanics Laboratory, University of California, Berkeley. A mixture of carbon tetrachloride, xylene (xylol) and zinc oxide was made, which had the same specific gravity as water. Droplets were injected into the water and the resulting motion was photographed through the glass sides of the channel with a motion picture camera. A clock and grid were placed in the field of view in order to obtain time and space coordinates. The motion pictures were analyzed frame by frame to obtain the data presented. The particle orbits for the deep-water and shallow-water waves were adjusted so that the apparent mass transport was eliminated. This was done by measuring the apparent mass transport over one wave cycle and apportioning the negative of this motion linearly over the particle path for one wave cycle. During all experiments with unbroken waves, the waves were made as steep as possible.

---

*Superscript numbers in parentheses refer to references at end of report

First and Second Approximations of Stokes Wave Theory: The first and second approximations of Stokes wave theory were compared with the measured wave surface time history, horizontal and vertical particle velocity and the particle path.

The second approximation of Stokes wave theory for the wave profile[1,2] is given by the expression

$$\frac{S}{d} = 1 + \frac{H}{2d}\left\{\cos\frac{2\pi\bar{x}}{L} + \frac{\pi H}{2L}\left[\frac{\cosh\frac{2\pi d}{L}\left(\cosh\frac{4\pi d}{L} + 2\right)}{2\left(\sinh\frac{2\pi d}{L}\right)^3}\right]\cos\frac{4\pi\bar{x}}{L}\right\} \qquad (1)$$

where

S = elevation of the particle above the bottom (ft.); in this case the surface particle
d = still-water depth (ft.)
H = wave height (ft)
$\bar{x}$ = horizontal distance from origin (the wave crest) to the particle (ft.)
L = wave length (ft.)
t = time (sec.)
T = wave period (sec.)

Equation (1) becomes the surface time history by replacing $\bar{x}/L$ with t/T which is possible for waves of permanent form. This was the only theory used for comparison with the measured surface time history because the trochoidal surface time history[3,4] and Stokes' deep water surface time history[1], all agree closely with each other and with the measured surface time history for deep water. In shallow water the previously mentioned expressions for the surface time history do not agree with each other nor with the experimental results. Furthermore, the third approximation of Stokes wave theory will only slightly improve the situation. The writer believes it would take many approximations to extend the Stokes wave theory to waves of appreciable steepness in very shallow water.

The first approximation (Stokes) to the horizontal particle velocity[1] is given by the expression

$$u = \frac{\pi H}{T}\,\frac{\cosh\frac{2\pi S}{L}}{\sinh\frac{2\pi d}{L}}\cos\theta \qquad (2)$$

where

u = horizontal particle velocity, (ft. per sec.)

θ = angular position of particle in its orbit measured counterclockwise and where there is no mass transport, (degrees)

The use of θ is a modification of the Stokes equation which includes the assumption that the horizontal particle velocity is zero at the mean vertical particle position. The use of θ applies only for the first approximation.

The second approximation (Stokes) of the horizontal particle velocity[1,2] is given by the expression

$$u = \frac{\pi H}{T} \frac{\text{Cosh}\,\frac{2\pi S}{L}}{\text{Sinh}\,\frac{2\pi d}{L}} \text{Cos}\,\frac{2\pi}{L}(\bar{x} + x - ct) + \frac{3}{4}\frac{\pi^2 H^2}{L\,T}\frac{\text{Cosh}\,\frac{4\pi S}{L}}{(\text{Sinh}\,\frac{2\pi d}{L})^4}\text{Cos}\,\frac{4\pi}{L}(\bar{x}+x-ct) \quad (3)$$

where

x = horizontal position of particle in its mean horizontal position (ft).

c = wave velocity of propagation, (ft/sec)

The particle velocity under the crest becomes

$$u\,(\text{crest}) = \frac{\pi H}{T}\frac{\text{Cosh}\,\frac{2\pi S}{L}}{\text{Sinh}\,\frac{2\pi d}{L}} + \frac{3}{4}\frac{\pi^2 H^2}{L\,T}\frac{\text{Cosh}\,\frac{4\pi S}{L}}{(\text{Sinh}\,\frac{2\pi d}{L})^4} \quad (4)$$

and the particle velocity under the trough becomes

$$u\,(\text{trough}) = \frac{-\pi H}{T}\frac{\text{Cosh}\,\frac{2\pi S}{L}}{\text{Sinh}\,\frac{2\pi d}{L}} + \frac{3}{4}\frac{\pi^2 H^2}{L\,T}\frac{\text{Cosh}\,\frac{4\pi S}{L}}{(\text{Sinh}\,\frac{2\pi d}{L})^4} \quad (5)$$

The absolute values of u (crest) and u (trough) and the maximum value of Equation (2) were compared to the measured horizontal particle velocities under the crest and trough of the waves. In deep water all the expressions gave the same close agreement. In shallow water for waves of appreciable steepness, Equation (2) (linear theory) compares more closely to the experimental results than the second approximation of the Stokes wave theory.

The second approximation (Stokes) to the vertical particle velocity[1] (v in ft./sec.) is given by the expression

$$v = \frac{\pi H}{T}\frac{\text{Sinh}\,\frac{2\pi S}{L}}{\text{Sinh}\,\frac{2\pi d}{L}}\text{Sin}\,\frac{2\pi}{L}(\bar{x} + x - ct) + \frac{3}{4}\frac{\pi^2 H^2}{L\,T}\frac{\text{Sinh}\,\frac{4\pi S}{L}}{(\text{Sinh}\,\frac{2\pi d}{L})^4}\text{Sin}\,\frac{4\pi}{L}(\bar{x}+x-ct) \quad (6)$$

which for the mean vertical particle position becomes

$$v = \pm\frac{\pi H}{T}\frac{\text{Sinh}\,\frac{2\pi S}{L}}{\text{Sinh}\,\frac{2\pi d}{L}} \quad (7)$$

This result is common to both the first and second approximations in deep or shallow water.

The second approximation (Stokes) to the horizontal particle position[1,2] in its orbit with no mass transport is given by the expression

$$x = \frac{-H}{2}\frac{\text{Cosh}\,\frac{2\pi S}{L}}{\text{Sinh}\,\frac{2\pi d}{L}}\text{Sin}\,\frac{2\pi}{L}(\bar{x}-ct) - \frac{\pi H^2}{4L\,(\text{Sinh}\,\frac{2\pi d}{L})^2}\left[-\frac{1}{2} + \frac{3}{4}\frac{\text{Cosh}\,\frac{4\pi S}{L}}{(\text{Sinh}\,\frac{2\pi d}{L})^2}\right]\text{Sin}\,\frac{4\pi}{L}(\bar{x}-ct) \quad (8)$$

Where S for this case is the mean particle elevation above the bottom, (ft.) Equation 8 seems almost entirely inadequate for all but a few values of $\frac{d}{L}$. In deep water and for better agreement in shallow water the equation was reduced to

$$x = -\frac{H}{2} \frac{\text{Cosh } \frac{2\pi S}{L}}{\text{Sinh } \frac{2\pi d}{L}} \text{ Sinh } \frac{2\pi}{L} (\bar{x} - ct) \qquad (9)$$

The second approximation (Stokes) to the vertical particle position (1,2) in its orbit is given by the expression

$$y = \frac{H}{2} \frac{\text{Sinh } \frac{2\pi S}{L}}{\text{Sinh } \frac{2\pi d}{L}} \text{ Cos } \frac{2\pi}{L}(\bar{x}-ct) + \frac{3}{16} \frac{\pi H^2}{L} \frac{\text{Sinh } \frac{4\pi S}{L}}{(\text{Sinh } \frac{2\pi d}{L})^4} \text{ Cos } \frac{4\pi}{L} (\bar{x} - ct) \qquad (10)$$

For shallow water Equation (10) becomes inadequate and better results were obtained when it was reduced to the following expression

$$y = \frac{H}{2} \frac{\text{Sinh } \frac{2\pi S}{L}}{\text{Sinh } \frac{2\pi d}{L}} \text{ Cos } \frac{2\pi}{L} (\bar{x} - ct) \qquad (11)$$

The sign, sine, and cosine convention used in the above equations are consistent with the figures presented in the report and may vary slightly from some of the references.

Results and Discussion: The experimental results are presented in graphical form. A summary of the wave conditions covered is presented in Table I. Figures 1 to 5 cover the conditions of $\frac{d}{L}$ greater than about 0.2. Figures 6 to 10, and 17 to 25 cover the conditions of $\frac{d}{L}$ less than 0.20. Figures 11 to 16 cover the case of breaking waves on sloping beaches. Since there can be no abrupt change from good agreement to bad agreement, Figures 5, 6 and 17 where values of d/L range between 0.20 to 0.10 may be classed as the region where the Stokes theory deviates 20% or more from the measurements for waves of appreciable steepness.

Figure 1 shows a very steep, deep-water wave (d/L = 0.556) where the theoretical results for the second approximation of the Stokes theory are approximately the same as for the first approximation. The maximum error between the theory and measurements is about 20% based on the measured results. The particle path for this wave condition is almost exactly a circle. Figure 2 where $\frac{d}{L}$ = 0.449 is almost identical with Figure 1, but with a wave that is somewhat less steep. Figure 3 shows a relatively steep wave in water that is relatively shallow (d/L = 0.238). The theoretical horizontal particle velocity shows the variation between the first and second approximations. The agreement between measurement and theory is generally within 20% based on the measured results for this case. Figure 4 (d/L = 0.228) is almost identical with Figure 3. The particle path in this case is now elliptical.

Figure 5 shows a very steep wave in relatively shallow water (d/L = 0.191) and is an example of the beginning of the deviation of the second approximation. The surface time history has a definitely flat trough for more than 60% of the wave cycle which is characteristic of shallow water waves of appreciable steepness. The horizontal particle velocity distribution shows less curvature than the steep wave shown in Figure 1. The data presented thus far on horizontal particle velocity indicate that the particle velocity at a given elevation above the bottom is the same magnitude under the crest as under the trough. The second approximation of the Stokes theory indicates that the variation between the trough horizontal particle velocity and the crest velocity at the same level should be about 20%. The point has now been reached where the difference between the first and second approximation is about the same as the difference between the measurements and the Stokes theory so that waves in more shallow water can be expected to show even greater variation between theory and measurement. For this example (Figure 5) the particle path is elliptical but is more rounded at the crest and flattened at the trough both in measurement and theory indicating typical shallow water effects. Another example of a wave in the same range is shown in Figures 6 and 17. This wave would not be considered steep in deep water, but it is a steep wave in this relatively shallow water (d/L = 0.110). The wave surface time history and horizontal particle velocity shows good agreement with the theory but in the latter case a definite increase in the difference between crest and trough velocity at the same level is shown.

Remarkably good agreement between the measured vertical particle velocity and the theoretical results is shown in Figure 17 for this wave condition. In the Figures 6 and 17 and in the following Figures 7 to 10 and 18 to 25, the waves were made as steep as possible for the shallow water condition presented.

Figures 7, 18 and 22 shows a relatively steep wave in relatively shallow water (d/L = 0.079) which is definitely beyond the region of good agreement. Any agreement of the measurements with the theory probably is more coincidental than anything else. For instance, the secondary wave shown in the theoretical profile of the second approximation (Figure 7a) is for a wave of permanent form, but the measured wave does not have a permanent form since the secondary wave is traveling at a different velocity than the large wave. The agreement between horizontal particle velocity and the theory is poor; however, there is considerable experimental scatter in this example (Figure 7b). Figures 7c, 22a, and 22b show fairly close agreement between theory and measurement, but the theory is a mixture of the first and second approximations. The first approximation is used in the x direction and the second approximation is used in the y-direction. Although the agreement is good, this approach is arbitrary in that using one approximation or the other depends upon a chosen d/L without any rules for this choice. If the second approximation is used in the x direction, the theoretical curve extends beyond the borders of the graph. The first approximation in the y-direction, if used alone, would mean a symmetrical orbit about y = 0. In Figure 18, the theory has departed considerably from the measured values of the vertical particle velocity. The wave illustrated in Figures 8, 19 and 23 is in slightly more shallow water (d/L = 0.057) than the wave of Figures 7, 18 and 22, but is otherwise identical. The theoretical surface time history differed so greatly from the measurements that it was considered not to apply and was not shown. In Figures 8b, 8c, 23a and 23b, only the first approximation was used and showed better agreement to the measurements than the second approximation which could not be contained within the graph. This close agreement of the first approximation is contradictory to the theoretical approach indicated in that the

second approximation should for all cases be better than the first approximation. Figure 19 of the vertical particle velocity for this wave shows that the theory lays within the experimental scatter.

The wave condition ($\frac{d}{L} = 0.044$) of Figures 9, 20 and 24, and the wave condition ($\frac{d}{L} = 0.035$) of Figures 10, 21, and 25 show such poor agreement with the Stokes wave theory that the theoretical curves could not be contained within the limits of the graphs except for the horizontal and vertical particle velocities. In Figure 10a, a secondary wave is shown traveling at almost half the velocity of the larger wave. In Figures 10c and 25, the secondary wave appears as an inner loop in the particle orbit. In Figure 9a, a slight secondary wave was shown and this causes the hesitant particle motion shown at the right side of Figures 9c and 24. In Figures 9b and 10b, the horizontal particle motion under the trough is definitely less than the particle velocity under the crest. Further, the maximum horizontal particle velocity at the crest of the wave has not begun to approach the order of magnitude of the wave velocity.

The experimental results of the breaking waves on a sloping beach and the experimental results of the waves in very shallow water show that the trends of the water particle motion of the shallow water waves are continued when the wave breaks. The breaking waves presented are classified by the beach slope and their deep-water steepness. Two beach slopes (1:10 and 1:50) were selected as about representative of the two extremes possible in the model. From the model study it was found that steep waves on a relatively steep beach plunged upon breaking while low waves spilled upon breaking. On a flat beach, the steep waves form spilling breakers and the low waves form plunging breakers. Figure 11 is an example of a very low wave on a steep beach. The surface time history is asymmetrical and very irregular. The irregular waves in the trough are traveling seaward. In Figure 11a, the surface time history and the space profile show good agreement over a distance of 20% of the wave length on either side of the crest. The horizontal particle velocity at the crest is approximately twice that at the bottom. However the maximum particle velocity under the trough is the same as under the crest at the same level. The maximum particle velocity near the crest is not as great as the wave velocity. The particle motion including mass transport is very irregular; however, it was observed within a relatively narrow region of the breaker that the maximum vertical particle velocity occurred as the wave crest approached and the maximum horizontal velocity occurred when the wave broke, even though the particle was not directly under the breaking crest. That is, the maximum horizontal particle velocity occurred at a position other than the maximum elevation in the orbit if the particle was not directly under the crest when the wave broke. Hence for such particles that were seaward of the breaker the maximum horizontal velocity occurred slightly afterward or exactly as the wave crest passed. For particles that were shoreward of the breaker maximum horizontal velocity occurred before the crest passed (foam line). The wave condition of Figure 12 is identical to that of Figure 11 except that the wave is steeper in deep water. For this wave the horizontal particle velocity at the crest is nearly the same as the wave velocity. Figure 13 shows a steep wave on a steep beach. This is the only breaking wave for which the Stokes theory was contained within the borders of the graph. Agreement between the breaker and the theory was not expected but it is interesting to find fair agreement as to the order of magnitude which was found for this case alone. Especially significant is that the horizontal particle velocity under the crest and trough are equal at equal levels. Hence steep waves on steep beaches behave more like waves in relatively deep water of constant depth than any other waves on sloping beaches. This is apparent if the facts are considered that a steep wave cannot shoal very much without breaking and that waves shoal rapidly in a short distance on steep beaches. Thus a steep wave on a steep beach cannot change much in shape before breaking.

Figure 14 shows a low wave on a flat beach. The surface time history is flat and long in the trough which is typical of very shallow-water waves. The horizontal particle velocity is typical of very shallow-water waves in that the velocity under the crests is about twice the particle velocity under the trough. The maximum particle velocity near the crest is nearly equal to the wave velocity. The particle path shows the very slow and hesitant motion of the trough set off from the very rapid motion as the crest passes and breaks. Figure 15 is a slightly steeper wave than Figure 14 but is otherwise identical. Figure 16 is that of a very steep wave on a flat beach. Again the phenomenon of Figure 15 is repeated. The profile is more symmetrical. The particle velocities under the crest and trough are equal. In this case the particle path is more regular or uniform. In Figure 15b and 16b, the maximum horizontal particle velocity near the crest is only half the wave velocity at breaking. This is evidence that only the slightest amount of water at the crest of the waves ever attains the velocity of wave propagation even at the breaking point. Figures 11a to 16a all showed that the surface time history ($x = 0$) passed the breaking point and the space profile ($t = 0$) show close agreement over a distance of about 20% of the wave length on either side of the breaking point.

Conclusions: The Stokes wave theory to the second approximation was compared to a wide range of model wave conditions. The waves were uniformly generated and progressed over constant depths and sloping beaches. From observation and comparison the following conclusions seem justified:

1. The theory and measurement for surface time histories or profiles, for vertical and horizontal particle velocities, and for particle orbits show agreement within 20% (based on the measured data) for all waves where $\frac{d}{L} > 0.2$.

2. There exists a range of $\frac{d}{L}$ between 0.2 and 0.1 where the theory shows fair agreement with the measurements of waves with appreciable steepness.

3. Where $\frac{d}{L} < 0.1$, the theory does not agree with the measurements either for waves in constant depth or for waves breaking on sloping beaches. It was not expected that the theory would compare with these very shallow-water waves.

4. In deep and relatively deep water the horizontal particle velocity under the crest and under the trough are equal in magnitude at the same elevation above the bottom. In shallow water the horizontal particle velocity under the crest may be about twice the magnitude as the particle velocity under the trough at the same level. Very steep waves on sloping beaches are similar to deep-water waves in regard to the fact that the horizontal particle velocity under the crest and trough are equal at the same level. Low waves on a low beach are similar to very shallow water waves in this respect.

5. The maximum horizontal particle velocity at the crest of the wave may attain the wave velocity of propagation as the wave breaks but this phenomenon is confined to a very narrow region of water at the crest of the wave.

6. Waves in very shallow water that form secondary waves are not waves of permanent form. The secondary wave travels at a velocity which is less than the velocity of the original wave train. The secondary wave causes a second loop in the particle orbit.

7. The surface time history and the space profile are nearly identical within a distance of about 20% of the wave length on either side of the crest of a breaking wave.

8. The maximum vertical particle velocity occurs at the mean particle position (y = 0). In the case of breaking waves on sloping beaches, the greatest maximum vertical velocity occurs as the wave crest approaches. The maximum horizontal particle velocity occurs under the crest when the wave passes or breaks. However, the maximum horizontal particle velocity may occur slightly before or slightly after the particle reaches the maximum elevation in its motion, that is slightly before or after the wave crest passes, depending on whether the particle is shoreward or seaward, respectively, of the breaker.

References

(1) Stokes, G.G. "On the Theory of Oscillatory Waves", Trans. Cambridge Philosophical Society, Vol. VIII, p. 441, 1947.

(2) Wiegel, R. L., and J. W. Johnson. "Elements of Wave Theory", Proceedings of First Conference on Coastal Engineering, 1951, Council on Wave Research, The Engineering Foundation.

(3) Beach Erosion Board. "A Summary of Progressive Oscillatory Waves in Water", Tech. Report No. 1, 1941, Corps of Engineers, Wash. D.C.

(4) Beach Erosion Board, "A Summary of the Theory of Oscillatory Waves", Tech. Report No. 2, 1942, Corps of Engineers, Wash. D.C.

Table I

Summary of Average Wave Conditions

Part I: Unbroken waves of constant height and period

Fig. No.	H ft.	L ft.	T sec.	C ft/sec	d ft.	H/L	d/L	Bottom Slope
1	0.362	3.76	0.87	4.34	2.09	0.096	0.556	Hor.
2	0.146	2.71	0.74	3.69	1.218	0.054	0.449	1:50
3	0.065	1.23	0.50	2.35	0.292	0.053	0.238	Hor.
4	0.297	5.17	1.06	5.06	1.181	0.057	0.228	1:50
5	0.469	5.42	1.22	4.44	1.035	0.087	0.191	Hor.
6	0.099	2.66	0.92	2.54	0.292	0.037	0.110	Hor.
7	0.150	3.71	1.30	3.02	0.292	0.031	0.079	Hor.
8	0.105	5.10	1.62	3.24	0.292	0.021	0.051	Hor.
9	0.131	6.56	2.11	2.99	0.292	0.020	0.044	Hor.
10	0.126	8.32	2.67	3.51	0.292	0.015	0.035	Hor

Part II: Breaking waves of constant period

Fig. No.	H_B ft.	T_B sec.	C_B ft/sec.	d_B ft.	H_o/L_o	Bottom Slope
11	0.24	2.50	5.45	0.252	0.0036	1:10
12	0.37	1.51	4.85	0.300	0.0208	1:10
13	0.35	1.00	3.55	0.423	0.0797	1:10
14	0.264	2.62	3.80	0.297	0.0037	1:50
15	0.276	1.41	4.00	0.350	0.0262	1:50
16	0.183	0.78	3.50	0.230	0.0778	1:50

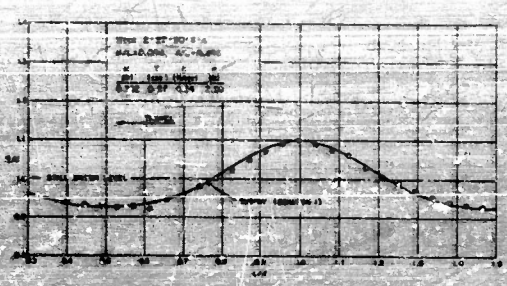

FIG. 1a - SURFACE TIME HISTORY

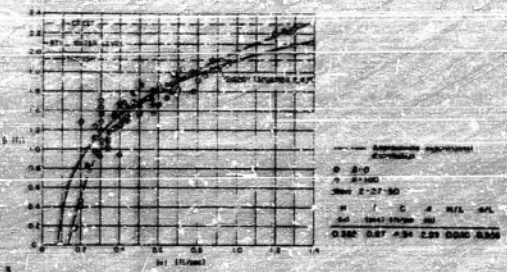

FIG. 1b - HORIZONTAL PARTICLE VELOCITY DISTRIBUTION

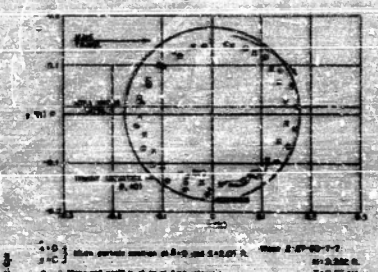

FIG. 1c - PARTICLE ORBIT ABOUT MEAN PARTICLE POSITION WITH NO MASS TRANSPORT

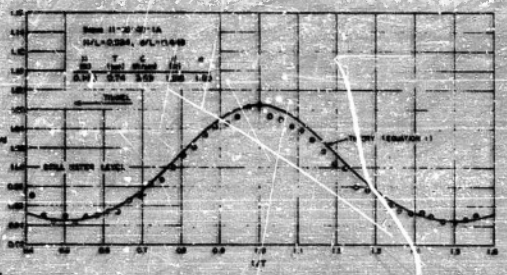

FIG. 2a - SURFACE TIME HISTORY

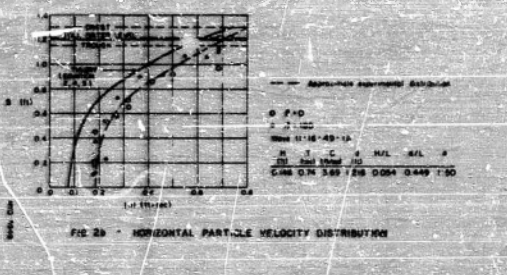

FIG. 2b - HORIZONTAL PARTICLE VELOCITY DISTRIBUTION

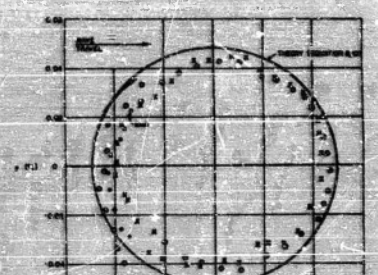

FIG. 2c - PARTICLE ORBIT ABOUT MEAN PARTICLE POSITION WITH NO MASS TRANSPORT

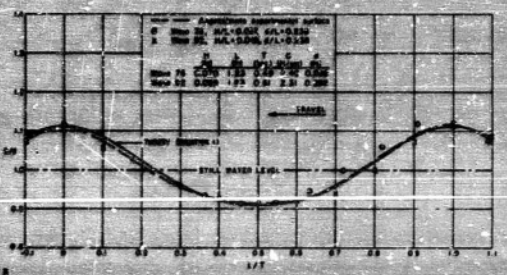

FIG. 3a - SURFACE TIME HISTORY

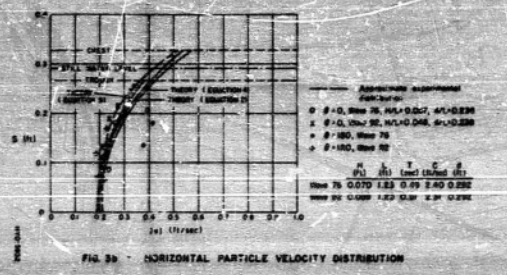

FIG. 3b - HORIZONTAL PARTICLE VELOCITY DISTRIBUTION

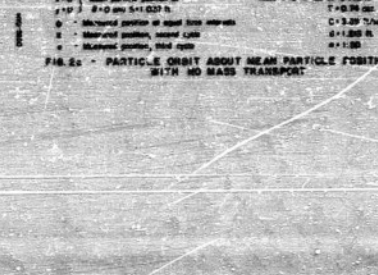

FIG. 3c - PARTICLE ORBIT ABOUT MEAN PARTICLE POSITION WITH NO MASS TRANSPORT

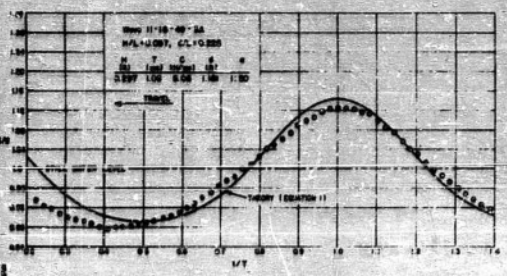

FIG. 4a - SURFACE TIME HISTORY

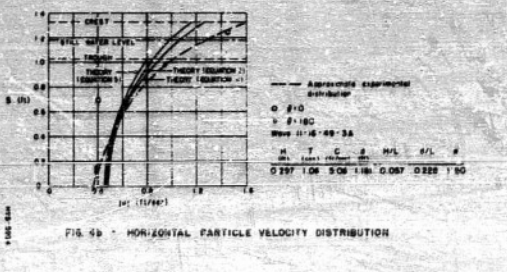

FIG. 4b - HORIZONTAL PARTICLE VELOCITY DISTRIBUTION

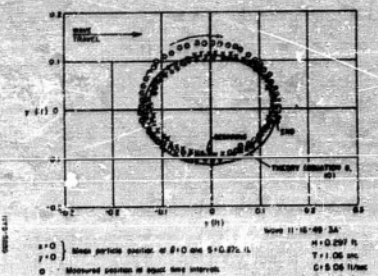

FIG. 4c - PARTICLE ORBIT ABOUT MEAN PARTICLE POSITION WITH NO MASS TRANSPORT

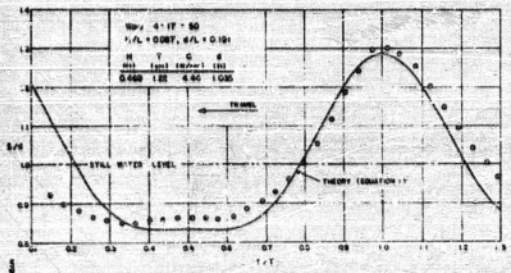

FIG. 5a - SURFACE TIME HISTORY

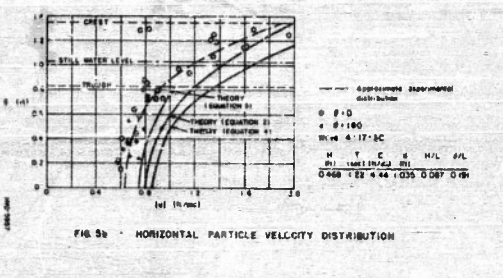

FIG. 5b - HORIZONTAL PARTICLE VELOCITY DISTRIBUTION

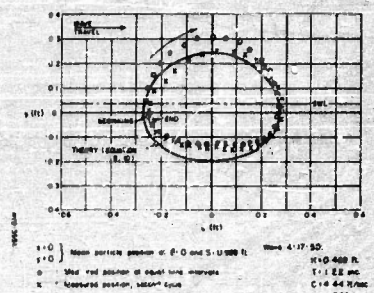

FIG. 5c - PARTICLE ORBIT ABOUT MEAN PARTICLE POSITION WITH NO MASS TRANSPORT

FIGURES 1a - 5c

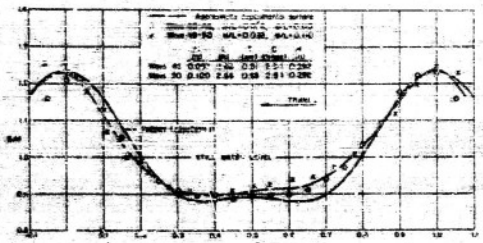

FIG. 4a - SURFACE TIME HISTORY

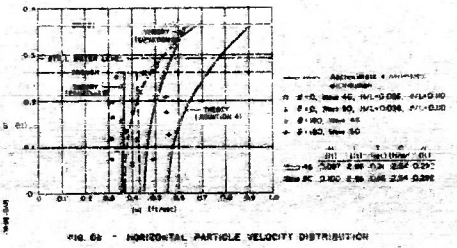

FIG. 6b - HORIZONTAL PARTICLE VELOCITY DISTRIBUTION

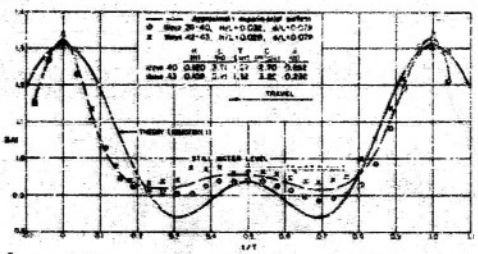

FIG. 7a - SURFACE TIME HISTORY

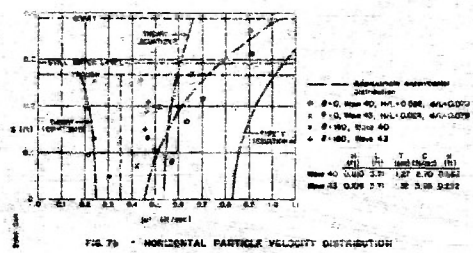

FIG. 7b - HORIZONTAL PARTICLE VELOCITY DISTRIBUTION

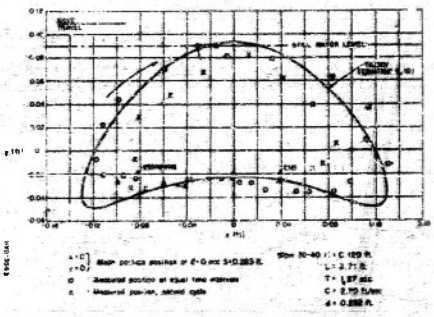

FIG 7c - PARTICLE ORBIT ABOUT MEAN PARTICLE POSITION WITH NO MASS TRANSPORT

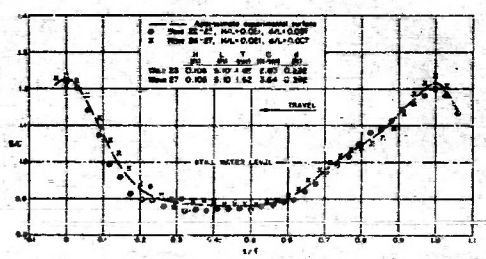

FIG 8a - SURFACE TIME HISTORY

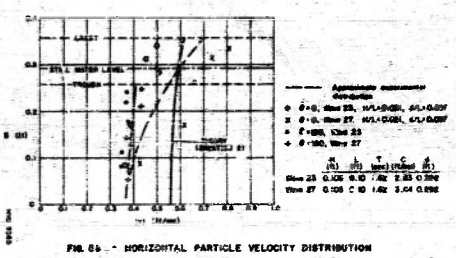

FIG. 8b - HORIZONTAL PARTICLE VELOCITY DISTRIBUTION

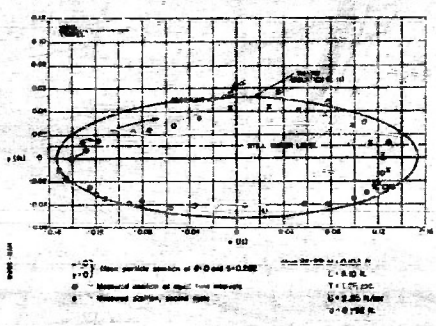

FIG. 8c - PARTICLE ORBIT ABOUT MEAN PARTICLE POSITION WITH NO MASS TRANSPORT

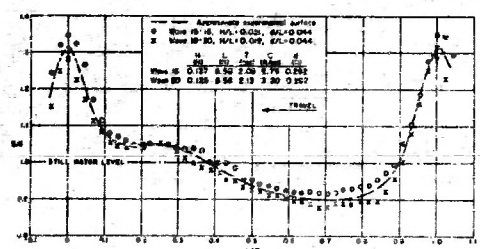

FIG 9a - SURFACE TIME HISTORY

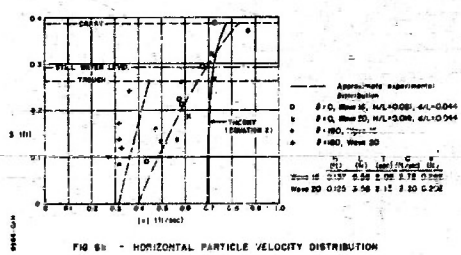

FIG 9b - HORIZONTAL PARTICLE VELOCITY DISTRIBUTION

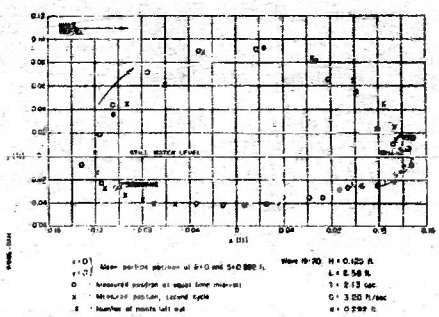

FIG 9c - PARTICLE ORBIT ABOUT MEAN PARTICLE POSITION WITH NO MASS TRANSPORT

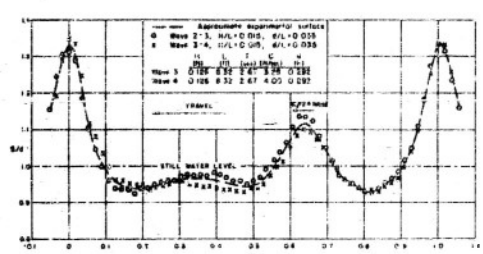

FIG 10a - SURFACE TIME HISTORY

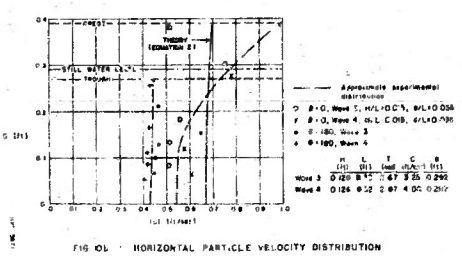

FIG 10b - HORIZONTAL PARTICLE VELOCITY DISTRIBUTION

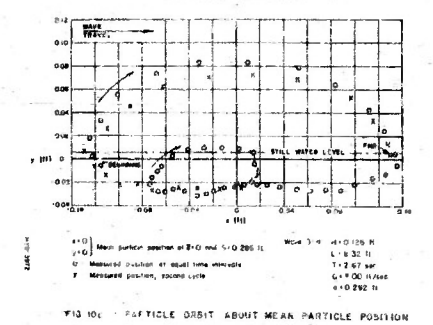

FIG 10c - PARTICLE ORBIT ABOUT MEAN PARTICLE POSITION WITH NO MASS TRANSPORT

FIGURES 6a - 10c

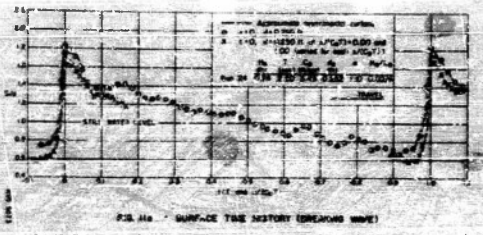

FIG. 11a - SURFACE TIME HISTORY (BREAKING WAVE)

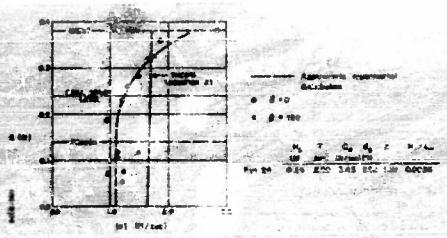

FIG. 11b - HORIZONTAL PARTICLE VELOCITY DISTRIBUTION (BREAKING WAVE)

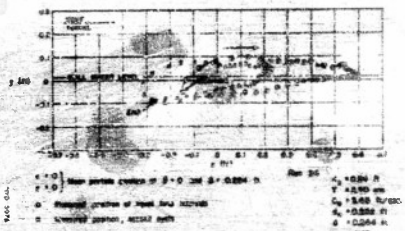

FIG. 11c - PARTICLE ORBIT ABOUT MEAN PARTICLE POSITION PATH MASS TRANSPORT (BREAKING WAVE)

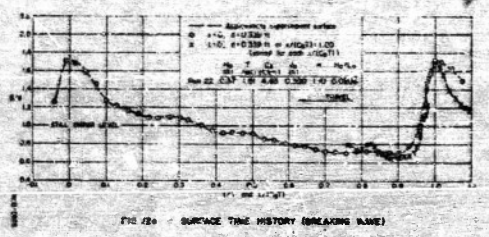

FIG. 12a - SURFACE TIME HISTORY (BREAKING WAVE)

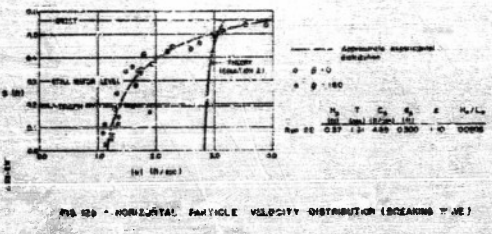

FIG. 12b - HORIZONTAL PARTICLE VELOCITY DISTRIBUTION (BREAKING WAVE)

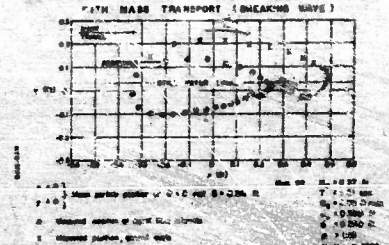

FIG. 12c - PARTICLE ORBIT ABOUT MEAN PARTICLE POSITION WITH MASS TRANSPORT (BREAKING WAVE)

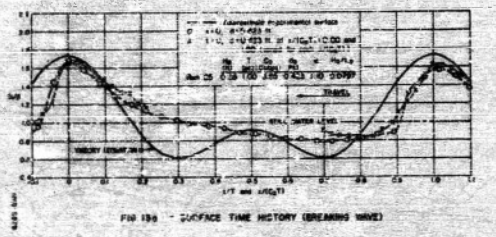

FIG. 13a - SURFACE TIME HISTORY (BREAKING WAVE)

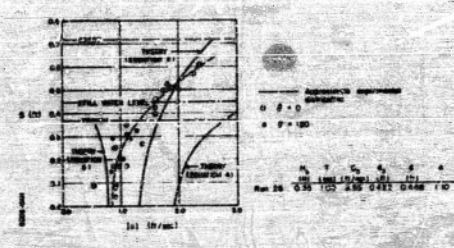

FIG. 13b - HORIZONTAL PARTICLE VELOCITY DISTRIBUTION (BREAKING WAVE)

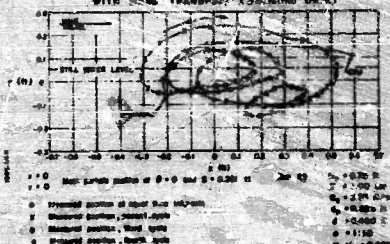

FIG. 13c - PARTICLE ORBIT ABOUT MEAN PARTICLE POSITION WITH MASS TRANSPORT (BREAKING WAVE)

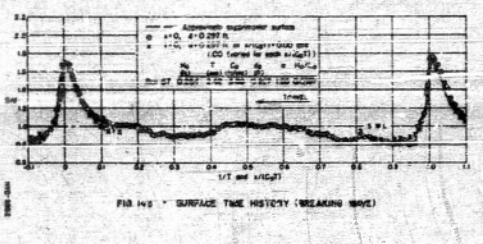

FIG. 14a - SURFACE TIME HISTORY (BREAKING WAVE)

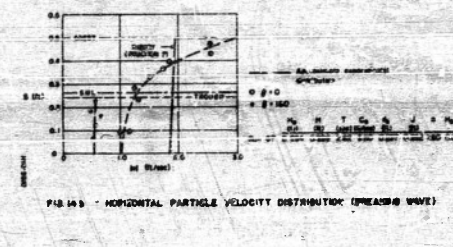

FIG. 14b - HORIZONTAL PARTICLE VELOCITY DISTRIBUTION (BREAKING WAVE)

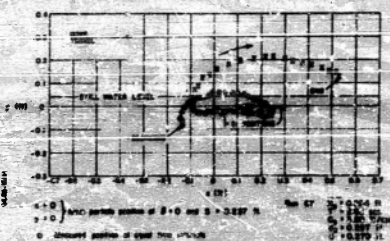

FIG. 14c - PARTICLE ORBIT ABOUT MEAN PARTICLE POSITION WITH MASS TRANSPORT (BREAKING WAVE)

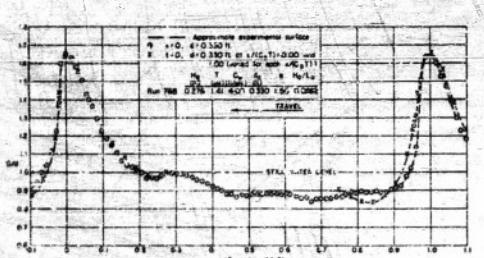

FIG. 15a - SURFACE TIME HISTORY (BREAKING WAVE)

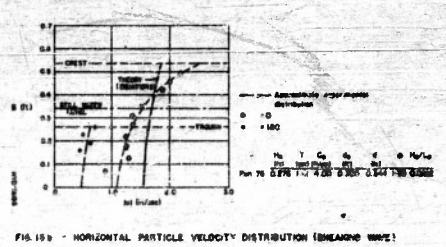

FIG. 15b - HORIZONTAL PARTICLE VELOCITY DISTRIBUTION (BREAKING WAVE)

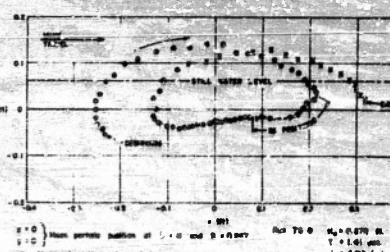

FIG. 15c - PARTICLE ORBIT ABOUT MEAN PARTICLE POSITION WITH MASS TRANSPORT

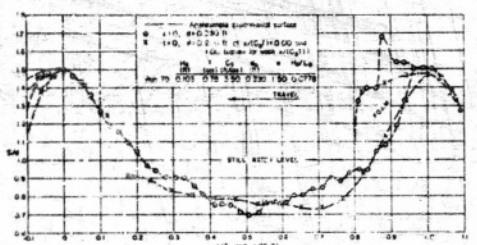

FIG. 16a - SURFACE TIME HISTORY (BREAKING WAVE)

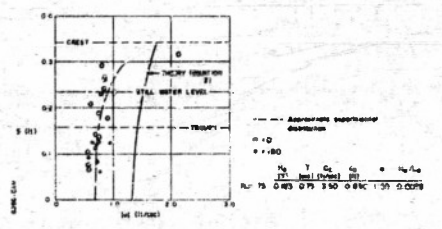

FIG. 16b - HORIZONTAL PARTICLE VELOCITY DISTRIBUTION (BREAKING WAVE)

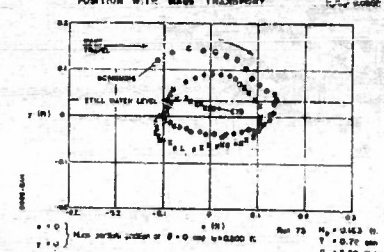

FIG. 16c - PARTICLE ORBIT ABOUT MEAN PARTICLE POSITION WITH MASS TRANSPORT (BREAKING WAVE)

FIGURES 11a - 16c

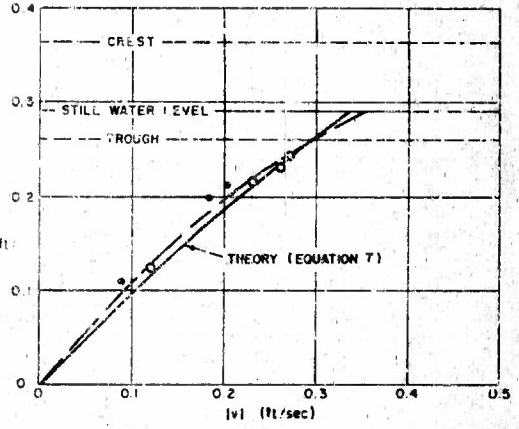

Approximate experimental distribution

- o θ=90°, Wave 46, H/L=0.036, d/L=0.110
- • θ=270°, Wave 46

	H (ft)	L (ft)	T (sec)	C (ft/sec)	d (ft)
Wave 46	0.097	2.66	0.91	2.54	0.292

FIG. 17 - VERTICAL PARTICLE VELOCITY DISTRIBUTION

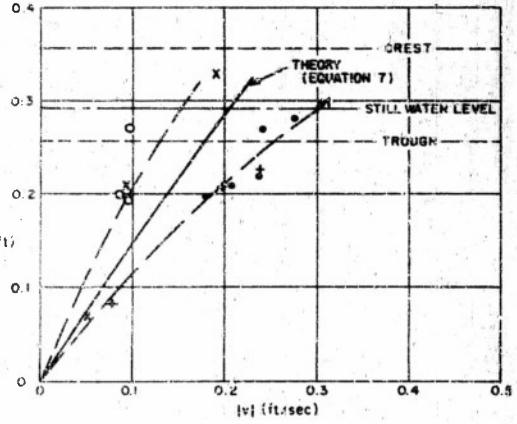

Approximate experimental distribution

- o θ=90°, Wave 23, H/L=0.021, d/L=0.057
- x θ=90°, Wave 27, H/L=0.021, d/L=0.057
- • θ=270°, Wave 23
- + θ=270°, Wave 27

	H (ft)	L (ft)	T (sec)	C (ft/sec)	d (ft)
Wave 23	0.106	5.10	1.62	2.83	0.292
Wave 27	0.105	5.10	1.62	3.64	0.292

FIG. 19 - VERTICAL PARTICLE VELOCITY DISTRIBUTION

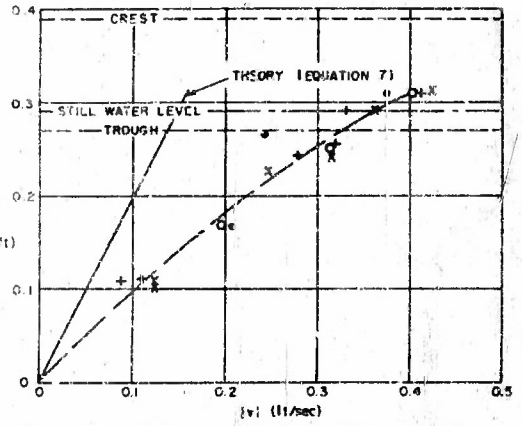

Approximate experimental distribution

- o θ=90°, Wave 3, H/L=0.015, d/L=0.035
- x θ=90°, Wave 4, H/L=0.015, d/L=0.035
- • θ=270°, Wave 3
- + θ=270°, Wave 4

	H (ft)	L (ft)	T (sec)	C (ft/sec)	d (ft)
Wave 3	0.126	8.32	2.67	3.25	0.2
Wave 4	0.126	8.32	2.67	4.00	0.2

FIG. 21 - VERTICAL PARTICLE VELOCITY DISTRIBUTION

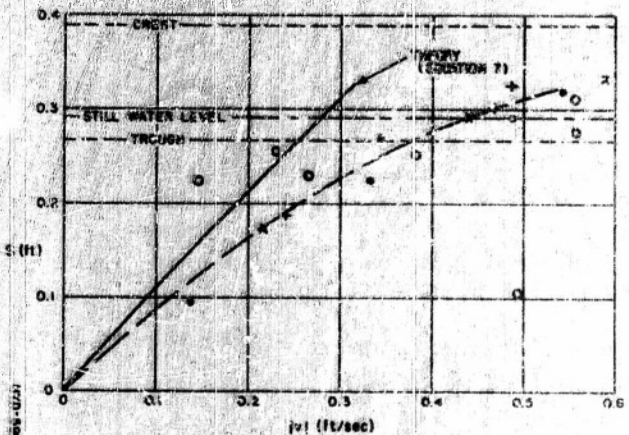

Approximate experimental distribution

- o θ=90°, Wave 40, H/L=0.032, d/L=0.079
- x θ=90°, Wave 43, H/L=0.029, d/L=0.079
- • θ=270°, Wave 40
- + θ=270°, Wave 43

	H (ft)	L (ft)	T (sec)	C (ft/sec)	d (ft)
Wave 40	0.120	3.71	1.27	2.70	0.292
Wave 43	0.109	3.71	1.32	3.25	0.292

FIG 18 - VERTICAL PARTICLE VELOCITY DISTRIBUTION

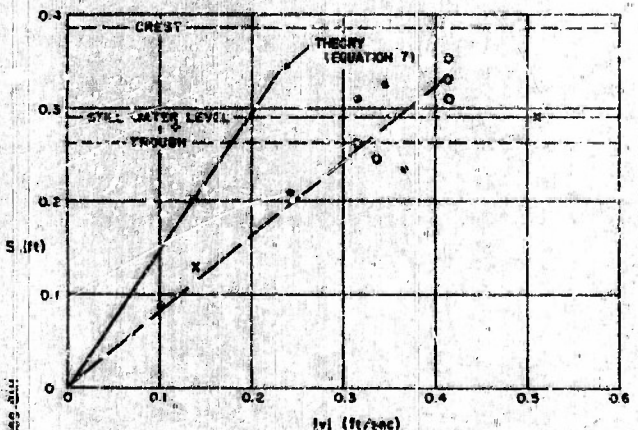

Approximate experimental distribution

- o θ=90°, Wave 16, H/L=0.021, d/L=0.044
- x θ=90°, Wave 20, H/L=0.019, d/L=0.044
- • θ=270°, Wave 16
- + θ=270°, Wave 20

	H (ft)	L (ft)	T (sec)	C (ft/sec)	d (ft)
Wave 16	0.137	6.58	2.09	2.78	0.292
Wave 20	0.125	6.58	2.13	3.10	0.292

FIG 20 - VERTICAL PARTICLE VELOCITY DISTRIBUTION

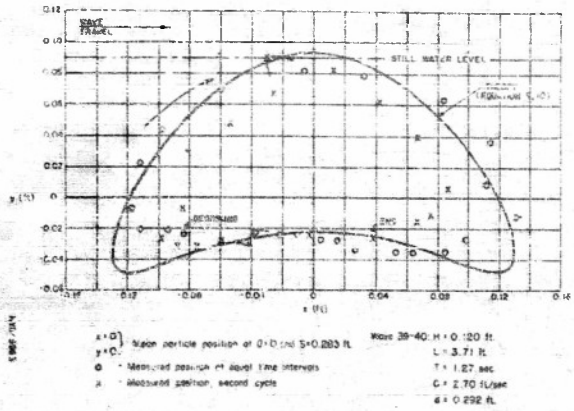

FIG 22a - PARTICLE ORBIT ABOUT MEAN PARTICLE POSITION WITH NO MASS TRANSPORT

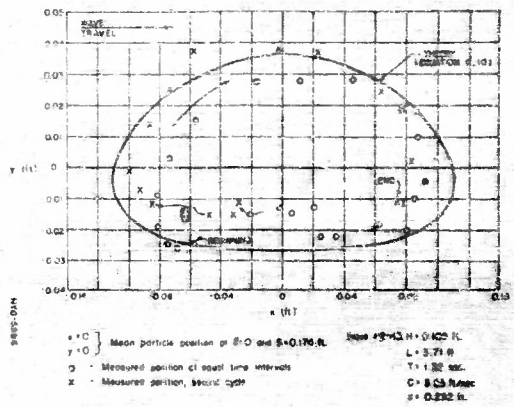

FIG 22b - PARTICLE ORBIT ABOUT MEAN PARTICLE POSITION WITH NO MASS TRANSPORT

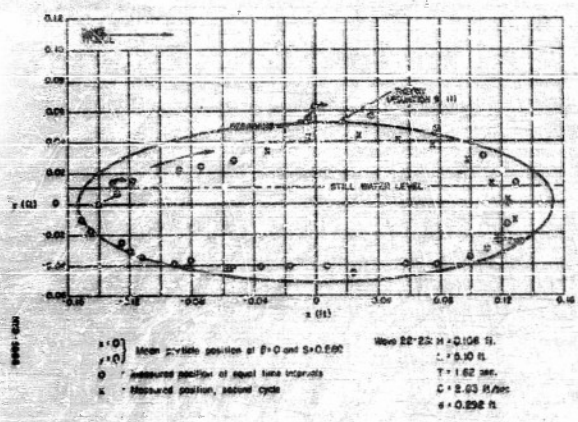

FIG 23a - PARTICLE ORBIT ABOUT MEAN PARTICLE POSITION WITH NO MASS TRANSPORT

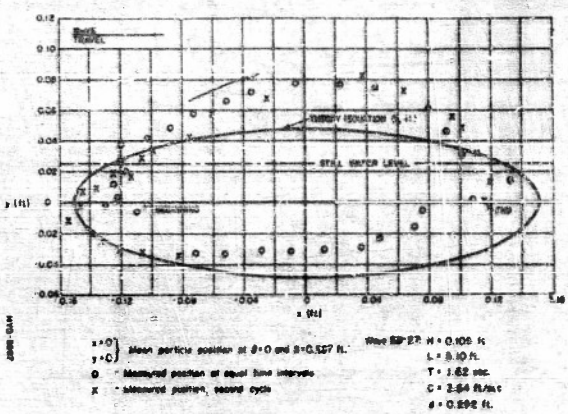

FIG 23b - PARTICLE ORBIT ABOUT MEAN PARTICLE POSITION WITH NO MASS TRANSPORT

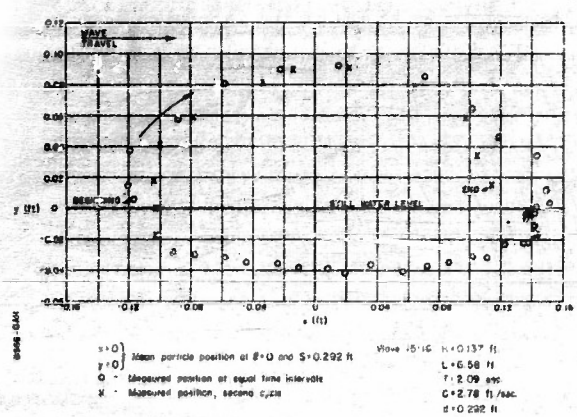

FIG 24a - PARTICLE ORBIT ABOUT MEAN PARTICLE POSITION WITH NO MASS TRANSPORT

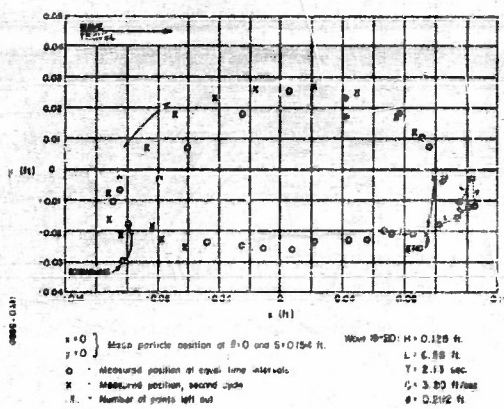

FIG 24b - PARTICLE ORBIT ABOUT MEAN PARTICLE POSITION WITH NO MASS TRANSPORT

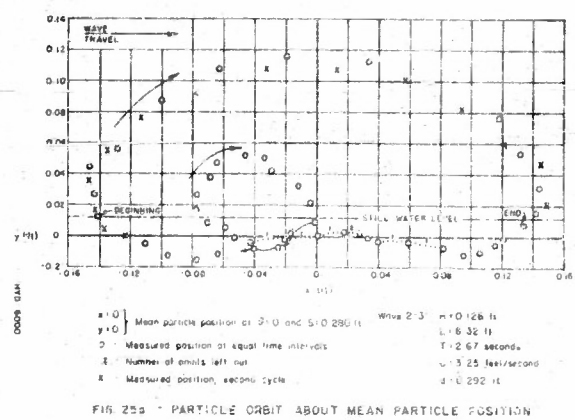

FIG 25a - PARTICLE ORBIT ABOUT MEAN PARTICLE POSITION WITH NO MASS TRANSPORT

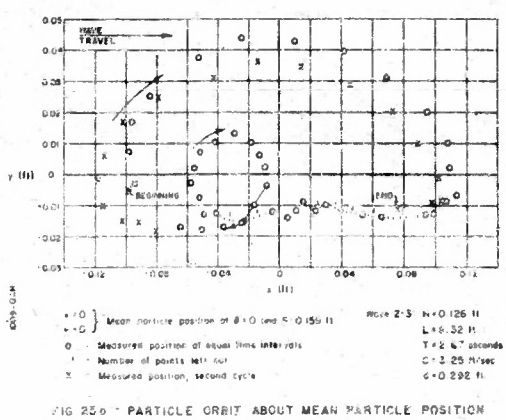

FIG 25b - PARTICLE ORBIT ABOUT MEAN PARTICLE POSITION WITH NO MASS TRANSPORT

DISTRIBUTION LIST

Technical Reports on Project NR 083-008

Copies	
13	Director Institute of Engineering Research University of California Berkeley 4, California
9	Naval Research Laboratory Technical Services Washington 25, D.C.
6	U.S. Navy Hydrographic Office Washington 25, D.C.
3	Chief of Naval Research Navy Department Washington 25, D.C. Attn: Code 416
3	British Joint Services Mission Main Navy Building Washington 25, D.C.
2	Asst. Naval Attache for Research American Embassy Navy Number 100 Fleet Post Office New York, New York
2	Director U.S. Naval Electronics Laboratory San Diego 52, California Attn: Code 550, 552
2	Director Woods Hole Oceanographic Institution Woods Hole, Massachusetts
2	Director Scripps Institution of Oceanography La Jolla, California
2	Director U.S. Fish & Wildlife Service Department of the Interior Washington 25, D.C. Attn: Dr. L.A. Walford
2	Chief, Bureau of Ships Navy Department Washington 25, D.C. Attn: Code 847

Copies	
1	Chief of Naval Research Navy Department Washington 25, D.C. Attn: Code 466
1	Director Office of Naval Research Branch Office 150 Causeway Street Boston Massachusetts
1	Director Office of Naval Research Branch Office 346 Broadway New York 13, New York
1	Director Office of Naval Research Branch Office 844 North Rush Street Chicago 11, Illinois
1	Director Office of Naval Research Branch Office 1000 Geary Street San Francisco 9, California
1	Director Office of Naval Research Branch Office 1030 East Green Street Pasadena 1, California
1	Chief, Bureau of Ships Navy Department Washington 25, D.C.
1	Commander Naval Ordnance Laboratory White Oak Silver Spring 19, Maryland
1	Commanding General Research & Development Divisio Department of the Army Washington 25, D.C.

1 Director of Research & Development
Hq. U.S. Air Force
AF DRD-RE-1
Washington 25, D.C.

1 Commanding Officer
Cambridge Field Station
230 Albany Street
Cambridge 39, Massachusetts
Attn: CRHSL

1 Commandant (OAO)
U.S. Coast Guard
1300 E Street, N.W.
Washington, D.C.

1 Chief, Bureau of Yards & Docks
Navy Department
Washington 25, D.C.

1 Chairman, Ship to Shore Continuing
Board, U.S. Atlantic Fleet
Commander, Amphibious Group 2
c/o Fleet Post Office
New York, New York

1 Commander, Amphibious Forces
Pacific Fleet
San Francisco, California

1 Commander
Amphibious Training Command
U.S. Pacific Fleet
San Diego 32, California

1 U.S. Army
Beach Erosion Board
5201 Little Falls Road, N.W.
Washington 16, D.C.

1 U.S. Waterways Experiment Station
Vicksburg, Mississippi

1 U.S. Engineers Office
San Francisco District
180 New Montgomery Street
San Francisco 19, California

1 U.S. Engineers Office
Los Angeles District
P.O. Box 17277, Foy Station
Los Angeles 17, California

1 U.S. Engineers Office
South Pacific Division
P.O. Box 3339, Rinson
Annex
130 Sutter Street
San Francisco, California

1 Office of Honolulu Area
Engineers
Corps of Engineers
U.S. Army
P.O. Box 2240
Honolulu, T.H.

1 Commandant of the Marine
Corps School
Quantico, Virginia

1 Sir Claude Inglis, CBE
Director of Hydraulics
Research
c/o Office of Naval Research
Branch Office
Navy No. 100, Fleet P.O.
New York, New York

1 Commanding Officer
U.S. Naval Civil Engineering
Research & Evaluation Lab.
Construction Battalion Center
Port Hueneme, California

1 Commandant, Marine Corps
Hq. Marine Corps
G-4, Room 2131
Arlington Annex
Washington, D.C.
Attn: Lt-Col. H.H. Riche

1 Chief, Air Weather Service
Andrews Air Force Base
Washington 25, D.C.
Attn: Mr. R. Stone

1 Research & Development Board
National Military Estab.
Washington 25, D.C.
Attn: Comm. on Geophysics
and Geography

1 National Research Council
2101 Constitution Avenue
Washington 25, D.C.
Attn: Comm. on Undersea
Warfare

1 Director
U.S. Coast & Geodetic Survey
Department of Commerce
Washington 25, D.C.

1 Department of Engineering
University of California
Berkeley 4, California

1 California Academy of Sciences
Golden Gate Park
San Francisco, California
Attn: Dr. R.C. Miller

1 Head, Dept. of Oceanography
Texas A & M
College Station, Texas

1 Director
Chesapeake Bay Institute
Box 426A, RFD #2
Annapolis, Maryland

1 Director
Lamont Geological Observatory
Torrey Cliff
Palisades, New York

1 Head, Dept. of Oceanography
University of Washington
Seattle 5, Washington

1 The Oceanographic Institute
Florida State University
Tallahassee, Florida

1 Director
Narragansett Marine Laboratory
Kingston, Rhode Island

1 Bingham Oceanographic Foundation
Yale University
New Haven, Connecticut

1 Department of Conservation
Cornell University
Ithaca, New York
Attn: Dr. J. Ayers

1 Allen Hancock Foundation
University of Southern California
Los Angeles 7, California

1 Director
Hawaii Marine Laboratory
University of Hawaii
Honolulu, T.H.

1 Director
Marine Laboratory
University of Miami
Coral Gables, Florida

1 Head, Dept. of Oceanography
Brown University
Providence, Rhode Island

1 Dept. of Zoology
Rutgers University
New Brunswick, New Jersey
Attn: Dr. H. Haskins

1 U.S. Fish & Wildlife Service
P. O. Box 3830
Honolulu, T.H.

1 U.S. Fish & Wildlife Service
Woods Hole, Massachusetts

1 U.S. Fish & Wildlife Service
Fort Crockett
Galveston, Texas

1 U.S. Fish & Wildlife Service
460 B. Jordan Hall
Stanford University
Stanford, California

1 U.S. Fish & Wildlife Service
South Atlantic Offshore
Fishery Investigations
c/o Georgia Game & Fish Comm.
P. O. Box 312
Brunswick, Georgia

1 Mr. A. L. Cochran
Chief, Hydrology & Hydr. Branch
Chief of Engineers
Gravelly Point
Washington, D.C.

1 District Engineer
Jacksonville District
Corps of Engineers, U.S. Army
575 Riverside Avenue
Jacksonville 1, Florida